Extracorporeal shockwaves (ESWs) enhance the osteogenic medium-induced differentiation of adipose-derived stem cells into osteoblast-like cells

Extracorporeal Shock Waves (ESW) enhance the osteogenic medium-induced differentiation of Adipose-derived Stem Cells into osteoblast-like cells

Short title: Osteogenic differentiation of stem cells by ESW

Maria Graziella Catalano[a], Francesca Marano[a], Letizia Rinella[a], Laura de Girolamo[b], Ornella Bosco[a], Nicoletta Fortunati[c], Laura Berta[d], Roberto Frairia[a]

[a]Department of Medical Sciences, University of Turin, Turin, Italy; [b]Orthopaedic Biotechnologies Laboratory, IRCCS Istituto Ortopedico Galeazzi, Milan, Italy; [c]Oncological Endocrinology, AO Città della Salute e della Scienza di Torino, Turin, Italy; [d]Med&Sport 2000 Srl, Turin, Italy.

Corresponding Author: Roberto Frairia, Department of Medical Sciences, University of Turin, Via Genova 3, 10126 Turin, Italy; tel. +39-0116705391; fax. +39-0116705366; mail: roberto.frairia@unito.it

Abstract

Human Adipose-derived Stem Cells (hASCs) are a promising cell type for bone tissue engineering, given their potential to differentiate into osteoblast-like cells. Interactions among biochemical and mechanical signals result in bone formation and repair. In this process stem cells have a crucial role. Extracorporeal Shock Waves (ESW) are acoustic waves capable of enhancing bone regeneration suggesting that ESW may induce some signals for mesenchymal progenitor maturation. The aim of the present work is to investigate the effects of ESW treatment on the differentiation of hASCs into osteoblast-like cells and to better clarify the mechanisms involved. hASCs were treated with ESW and osteogenic medium; the effects in terms of gene expression, alkaline phosphatase (ALP) activity and calcium deposition were then evaluated. Moreover, to investigate the mechanisms of ESW action, reactive oxygen species (ROS) production, extracellular-signal-regulated kinases (ERK) and small 'mothers against' decapentaplegic (Smad) phosphorylation, and bone morphogenetic protein 2 (BMP2) expression were assessed. ESW treatment increased Runt related transcription factor 2 (Runx2), ALP and BMP2 expression, as well as ALP activity and calcium deposits with respect to untreated cells. Moreover ESW induced ROS formation, and both ERK and Smad phosphorylation. Our study shows the effects of ESW on osteogenic differentiation in an *in vitro* model using human adipose-derived stem cells and defines the mechanisms involved in this process. Our observations suggest that the combination of autologous hASCs and ESW treatment may improve bone tissue repair in tissue engineering procedures.

Key words: Extracorporeal Shock Waves, ESW, Adipose-derived Stem Cells, ASC, bone, osteogenic differentiation.

1. **INTRODUCTION**

Extensive bone loss due to trauma, inflammation and neoplasia are still a major clinical issue. The goal of bone tissue engineering is to enhance the regenerative ability of damaged bone as well as to identify novel cell-based therapies when repair processes are deficient. Human mesenchymal stem cells (MSCs) are a promising candidate cell type for musculoskeletal regenerative tissue engineering due to their capacity for self-renewal and multipotent differentiation. In fact, under specific conditions, MSCs are able to differentiate into bone, cartilage, and tendon (Pountos and Giannoudis, 2005). To date the majority of cell-based tissue regenerative protocols have involved the use of bone marrow MSCs; however, only a limited supply of cells can be obtained from bone marrow harvesting. In 2001, Zuk *et al*. first demonstrated that multilineage mesenchymal progenitor cells, similar to those obtained from bone marrow, are present in adipose tissue (Zuk *et al.*, 2001). Human adipose tissue represents a good candidate source of adult stem cells (human Adipose-derived Stem Cells, hASCs) because it is available in large quantities and can be collected by liposuction, not such an invasive procedure. Bone formation and repair are the result of interaction among biochemical and mechanical signals. Both processes involve the expression of multiple soluble and intracellular factors in a coordinated cascade of events. The musculoskeletal system responds to the loading environment and mechanical loading influences biological tissues (Maul *et al.*, 2011; Soucacos *et al.*, 2008). Extracorporeal Shock Waves (ESW) are transient short-term acoustic pulses with high peak pressure and a very short rise time to peak pressure on the order of magnitude of nanoseconds (one billionth of a second) and short pulse duration. ESW technology has been used in clinical practice since the 1980s, when lithotripters were first employed to break up kidney stones

(Sturtevant, 1996). More recently, shockwave therapy has emerged as a leading choice in the treatment of several orthopedic diseases (Wang, 2012a); in bone disorders, ESW treatment is being used successfully for non-union and delayed union of long bone fractures (Elster *et al.*, 2010; Xu *et al.*, 2009; Wang *et al.*, 2001; Rompe *et al.*, 2001) and for avascular necrosis of the femoral head (Alves *et al.*, 2009; Chen *et al.*, 2009; Wang *et al.*, 2012b). Experimental studies in animals have shown that ESW have osteogenic potential on damaged bone and promote bone union of segmental defect in rats (Wang *et al.*, 2003; Chen *et al.*, 2004a; Chen *et al.*, 2004b); ESW induce new bone formation in rabbits (Tischer *et al.*, 2008); they have anabolic effects in normal (van der Jagt *et al.*, 2011) and in osteoporotic rat bone (van der Jagt *et al.*, 2013); at osteotendinous junction with delayed healing they induce osteogenesis (Qin *et al.*, 2010), indicating that the bone microenvironment is responsive to physical ESW stimulation. Interestingly, it has been reported that ESW stimulate both the recruitment and the osteogenic differentiation of stem cells (Chen *et al.*, 2004b), and increase proliferation and differentiation of MG-63 human osteoblast-like cells by modifying ion channel activity without interfering with normal cell activity (Muzio *et al.*, 2010).

Although it has already been demonstrated that ESW drive progenitor cell differentiation towards osteogenic cell lineages through the production of TGFβ and VEGF (Wang *et al.*, 2002a, Chen *et al.*, 2004b) and oxygen radicals (Wang *et al.*, 2002b), the molecular mechanisms by which ESW exert their action are far from being fully understood.

The aim of the present study was to investigate the effects of ESW treatment on the differentiation of human adipose derived stem cells into osteoblast-like cells and to further explore the possible mechanisms involved in this process.

2. MATERIALS AND METHODS

2.1. hASC isolation, characterization and osteogenic differentiation.

hASCs were isolated from the subcutaneous-adipose tissue of 5 healthy female donors (range 30–50 yrs, BMI < 30 without any pathological obesity), undergoing elective liposuction, after written consent and Institutional-Review Board authorization. Primary cultures were established as follows: after digestion of raw lipoaspirates (50–100 ml) with 0.075% type I collagenase for 30 minutes, hASCs were separated by centrifugation (2100×g for 10 min), filtered and plated in basal medium (D-MEM/F12 plus 10% FBS). hASCs at passage 4 were investigated by flow cytometry analysis for the expression of several antigens using the following phycoerythrin (PE) or fluorescein isothiocyanate (FITC)-conjugated antibodies: mouse anti-human CD13, CD14 and CD34 (BD Biosciences, Fraklin Lakes, NJ, USA); mouse anti-human CD45, CD90, CD105, and CD44 (Immunotech, Marseille, France). Ten thousand events were acquired for each surface marker on flow cytometer (EPICS XL, Coulter Corp., Hialeah, FL).

To induce osteo-differentiation, hASCs were cultured in osteogenic medium consisting of basal medium supplemented with 10 mM glycerol-2-phosphate, 10 nM dexamethasone, 150 μM ascorbic acid-2-phosphate, and 10 nM cholecalciferol (de Girolamo *et al.*, 2007). hASCs cultured in basal medium were used as controls.

2.2. ESW treatment

The shock wave generator utilized for the *in vitro* experiments is a piezoelectric device (Piezoson 100, Richard Wolf, Knittlingen, Germany) especially designed for clinical use in orthopedics and traumatology. The experimental set-up has been previously reported (Frairia *et al.*, 2003). Briefly, aliquots of 1 ml of cell suspension adjusted to 1 x 10^6 cell/ml were placed in 20 mm polypropylene tubes (Nunc, Wiesbaden, Germany)

which were then completely filled with culture medium. Subsequently, cells were gently pelleted by centrifugation at 250 x *g* in order to minimize motion during shock wave treatment. Each cell-containing tube was placed in vertical alignment with the focal area and was adjusted so that the central point of the focal area corresponded to the centre of the tube bottom. The shock wave unit was kept in contact with the cell containing tube by means of a water-filled cushion. Common ultrasound gel was used as a contact medium between cushion and tube. Cells were treated as follows: 1) control cells receiving no ESW treatment and maintained in D-MEM/F12 plus FBS 10% (DMEM); 2) ESW-treated cells (EFD =0.32 mJ/mm^2; 1000 shots, peak positive pressure 90 MPa) receiving a number of 1000 shots (frequency = 4 shocks per second) and maintained in D-MEM/F12 plus FBS 10% (DMEM ESW); 3) cells receiving no ESW treatment and maintained in osteogenic medium (OST); 4) ESW-treated cells (EFD =0.32 mJ/mm^2; 1000 shots) maintained in osteogenic medium (OST ESW).

2.3. Cell viability

After treatment, cells were seeded at 3 x 10^3 cells/well in 96-well plates (Corning, New York, NY, USA). At 3, 6 and 10 days, cell viability was assessed using the Cell Proliferation Reagent WST-1 (Roche Applied Science, Penzberg, Germany), following the manufacturer's instructions. This is a colorimetric assay for the quantification of cell viability and proliferation, based on cleavage of the tetrazolium salt WST-1 by mitochondrial dehydrogenases in viable cells. Briefly, 10 μl of WST-1 were added to each well. After a 1 hour incubation, absorbance at 450 nm was measured using a plate reader (Model 680 Microplate Reader, Bio-Rad, Hercules, CA, USA). Four replicate wells were used to determine each data point.

2.4. Gene expression

At defined times after treatment, total RNA was extracted using TRIzol Reagent (Invitrogen Ltd, Paisley, UK). DNase I was added to remove remaining genomic DNA. 1 μg of total RNA was reverse-transcribed with iScript cDNA Synthesis Kit (Bio-Rad Laboratories Inc., Hercules, CA, USA), following manufacturer's protocol. Primers (Table 1) were designed using Beacon Designer 5.0 software according to parameters outlined in the Bio-Rad iCycler Manual. Specificity of primers was confirmed by BLAST analysis. Real-time PCR was performed using a BioRad iQ iCycler Detection System (Bio-Rad Laboratories Inc., Hercules, CA, USA) with SYBR green fluorophore. Reactions were performed in a total volume of 25 μl containing 12.5 μl IQ SYBR Green Supermix (Bio-Rad Laboratories Inc., Hercules, CA, USA), 1 μl of each primer at 10 μM concentration, and 5 μl of the previously reverse-transcribed cDNA template. The protocol used is as follows: denaturation (95°C for 5 min), amplification repeated 40 times (95°C for 15 sec, 60°C for 30 sec). A melting curve analysis was performed following every run to ensure a single amplified product for every reaction. All reactions were carried out at least in triplicate for each sample. Results were normalized using the geometric mean for three different housekeeping genes (β-actin, β2-microglobulin and L13A) and expressed as relative expression fold *versus* untreated controls.

2.5. Alkaline Phosphatase activity

Alkaline Phosphatase (ALP) activity, as described elsewhere (Maroni *et al.*, 2012), was measured in cell lysates (0.1% Triton X-100), using as substrate 1 mM p-nitrophenylphosphate in alkaline buffer (100 mM diethanolamine and 0.5 mM $MgCl_2$,

pH 10.5), and evaluating the absorbance at 405 nm on a multiplate reader (Model 680 Microplate Reader, Bio-Rad).

2.6. Alizarin Red Staining

Calcium deposition was measured by staining with 40 mM Alizarin Red-S (ARS, pH 4.1). After fixation in ethanol and washing with Tris-buffered saline, cells were stained with ARS for 15 minutes, washed with Tris-buffered saline, and observed under light microscope. Thereafter, calcium content was quantitatively analysed as previously described (Maroni *et al.*, 2012). Briefly, ARS was destained with 10% cetylpyridinium chloride (Sigma–Aldrich, Saint Louis, MO, USA) in 10 mM sodium phosphate buffer for 15 min at room temperature. Calcium content was determined by the absorbance measurement on a multiplate reader at 550 nm (Model 680 Microplate Reader, Bio-Rad).

2.7. Immunoblotting

At different times after treatments, cells were scraped from the flask in the presence of 1 ml lysis buffer (50 mM Tris–HCl pH 7.5, 150 mM NaCl, 1 mM EDTA, 1 mM EGTA, 0.5% sodium deoxycholate, 1% Nonidet P-40, 0.1% SDS, 10 mg/ml PMSF, 30 ml/ml aprotinin and 100 mM sodium orthovanadate). Cell lysates were incubated in ice for 30–60 min. At completion, tubes were centrifuged at 4 °C for 20 min at 15,000 × g. Clear supernatants were stored at −80 °C until use. For the assay, 4 μg of anti-total ERK 1/2 antibody (Upstate Biotechnology, Lake Placid NY, USA) were incubated with 100 μl of a slurry of 50% protein A agarose beads (Sigma–Aldrich, Saint Louis, MO, USA) for 30 min at 4 °C. Cell extracts containing 1 mg total protein per sample were precipitated with the beads for 2 h at 4 °C. Precipitated immunocomplexes were

separated on SDS-PAGE, transferred to PVDF and probed with monoclonal antibodies anti-phospho (Upstate Biotechnology, Lake Placid, NY, USA) and anti-total ERK 1/2 antibodies. Chemioluminescence detection was performed following ECL manufacturer's instructions. Bands were photographed and their intensity analysed with 1D Kodak Digital Science software.

2.8. Immunofluorescence microscopy

After treatment, cells (3 x 10^5) were seeded in 6 cm dishes. After 6 hours, cells were first put in acetone/methanol (1:1) at -20 °C for 20 minutes, washed with PBS containing 0.5% Triton X-100, 0.05% NaN_3 and incubated with anti-phospho-Smad 1/5/8 (mouse, Santa Cruz Biotechnology Inc, Santa Cruz, CA, USA), or anti-total-Smad 1/5/8 (mouse, Santa Cruz Biotechnology Inc, Santa Cruz, CA, USA) antibodies at 4°C overnight. Then cells were washed with PBS containing 0.5% Triton and 0.05% NaN_3 for 10 minutes for three times followed by detection with anti-mouse cy3 conjugated secondary antibodies, (GE Healthcare Europe, GmbH, Milan, Italy) in PBS plus 0.5% Triton and 0.05% NaN_3 for 2 hours. Nuclear staining was obtained by treating cells with Hoechst 33258 (500ng/ml in DMSO) in PBS. Cells were washed twice with distilled water and mounted with 50% glycerol-PBS media.

2.9. Intracellular ROS determination

Reactive oxygen species (ROS) were measured using 2',7'-dichloro-fluorescein (DCFH) diacetate as a probe (Canaparo *et al.*, 2006). Adherent cells were incubated with 5 μM DCFH for 30 minutes at 37°C in the dark. Intracellular ROS levels were measured using a flow cytometer (EPICS XL, Coulter Corp., Hialeah, FL).

2.10. Statistical Analysis

Data are expressed throughout the text as means ± SD. The means were calculated from at least three different experiments, each from different donors. Comparison between groups was performed with analysis of variance (two-way ANOVA) and the threshold of significance was calculated with the Bonferroni test. Statistical significance was set at $p<0.05$.

3. **RESULTS**

3.1. hASC characterization and ESW effect on cell viability

More than 95% of hASCs expressed CD13, CD44 and CD105, whereas a very low expression of CD14 (1-4%) and no expression of CD34 and CD45 was detected. Moreover, a positivity of at least 95% for the same markers was also maintained in subsequent steps (data not shown).

The energy level and number of shots used for ESW treatment (EFD =0.32 mJ/mm^2; peak positive pressure 90 MPa, 1000 shots) permitted a viability > 80% and no significant difference in terms of cell growth was observed between ESW treated and untreated cells, up to 10 days after treatment (supplementary figure 1).

3.2. ESW affect early osteogenic gene expression and alkaline phosphatase activity

As reported in figure 1, 72 h after treatment, ESW and osteogenic medium determined, even if used alone, a significant increase of Runx2 (panel A, DMEM ESW *vs* DMEM: 1.3 times, $p<0.05$; OST *vs* DMEM: 1.9 times, $p<0.01$) and ALP (panel B, DMEM ESW *vs* DMEM: 2.2 times, $p<0.01$; OST *vs* DMEM: 3.8 times, $p<0.001$) gene expression, though the greatest effect was achieved using the osteogenic medium/ESW combined treatment (for Runx2, panel A: OST ESW *vs* DMEM: 3.5 times, $p<0.001$; OST ESW *vs* OST: 1.9 times, $p<0.01$; for ALP, panel B: OST ESW *vs* DMEM: 6.6 times, $p<0.001$; OST ESW *vs* OST: 1.6 times, $p<0.01$). The enzymatic ALP activity confirmed the gene expression data (figure 1, panel C); once more, the combined treatment had the greatest effect (DMEM ESW *vs* DMEM: 1.4 times, $p<0.05$; OST *vs* DMEM: 1.8 times, $p<0.01$; OST ESW *vs* OST: 1.4 times, $p<0.01$; OST ESW *vs* DMEM: 2.6 times, $p<0.001$).

3.3. ESW affect mineralization

To further confirm the differentiation into osteoblasts induced by ESW and osteogenic medium, the presence of calcium deposits produced by differentiating cells was determined (figure 2, panels A and B). 28 days after treatment, calcium deposits, revealed by Alizarin Red staining, were observed both in cells treated with only ESW (figure 2, panel A-II) and with osteogenic medium alone (figure 2, panel A-III). However, again, the combined treatment (OST ESW) had the greatest effect (figure 2, panel A-IV), confirming the results of gene expression and ALP activity. Quantification of ARS (figure 2, panel B) confirmed the significant increase in calcium deposits already in the cells treated with ESW alone (DMEM ESW *vs* DMEM, $p<0.01$). Osteogenic medium determined a further increase in calcium deposits (OST *vs* DMEM, $p<0.001$), but it was the combined treatment with osteogenic medium and ESW which had the greatest effect (OST ESW *vs* DMEM, $p<0.001$; OST ESW *vs* OST, $p<0.05$).

3.4. ESW determine ROS production

Since it has been reported that ESW treatment, through reactive oxygen species production, induces osteogenic differentiation of bone marrow-derived mesenchymal stem cells (Wang *et al.*, 2002b), we determined ROS production after ESW treatment in hASCs. As reported in figure 3, panel A, 1 minute after ESW treatment, a significant increase in ROS production was already observed both in control and osteogenic medium, with respect to no ESW treatment (DMEM ESW *vs* DMEM: 11.5 times, $p<0.001$; OST ESW *vs* OST: 11.6 times, $p <0.001$). The increase was maintained until 5 min after treatment (DMEM ESW *vs* DMEM: 9.4 times, $p <0.001$; OST ESW *vs* OST: 12.3 times, $p <0.001$) but was not evaluable at successive times (determined up to 1

hour), where an increase was also observed in the samples not treated with ESW with respect to untreated cells at 1 minute (data not shown).

3.5. ESW activate ERK1/2 to induce osteogenic differentiation

Since ROS are able to determine ERK phosphorylation (Wang *et al.*, 2002b), we evaluated the effect of ESW on ERK1/2 phosphorylation level. As reported in figure 3, panel B, an increase in ERK 1/2 phosphorylation was already observed 15 minutes after ESW treatment in both basal conditions (DMEM ESW *vs* DMEM, $p < 0.05$) and in osteogenic medium (OST ESW *vs* DMEM, $p < 0.05$). The increase in ERK phosphorylation levels induced by ESW returned to basal condition levels after 60 min. The rapid and transient activation of this signaling cascade pathway suggests a response directly elicited by the mechanical stimulus. A similar effect has already been reported as result of mechanical strength in myocites and cardiomyocites (Rauch *et al.*, 2008; Komuro *et al.*, 1996).

3.6. ESW determine Smad phosphorylation

BMP2 signaling regulates osteogenic differentiation, acting through the Smad pathway (Phimphilai *et al.*, 2006; Liu *et al.*, 2011). In our *in vitro* model ESW determined the induction in BMP2 expression (DMEM ESW vs DMEM: 14 times, $p<0.001$; OST ESW vs OST: 20 times, $p<0.001$) (figure 4, panel A). Moreover, ESW treatment determined the nuclear localization of Smad (arrows, figure 4, panel B) which is the phosphorylated active form (arrows, figure 4, panel C).

4. DISCUSSION

In the present paper we have shown that extracorporeal shockwave treatment can promote and improve osteogenic medium-induced differentiation into osteoblast-like cells of adipose-derived stem cells. The evaluation of mesenchymal expression markers showed that the hASCs we isolated met the criteria of mesenchymal stem cells. Moreover, the fact that the same markers were also positive in subsequent steps guaranteed that the cells preserved their initial characteristics as long as they were used. The present paper confirmed the effect of a well characterized medium (de Girolamo et al., 2007; Maroni *et al.*, 2012) on osteoblast gene expression, ALP activity and calcium deposits. The novelty of the present work is the ability of ESW to promote the process of hASC differentiation even when used alone, and to boost the process of differentiation induced by the osteogenic medium. In fact, ESW treatment without any biochemical supplement determined a significant increase in Runx2, ALP and BMP2 expression as well as an increase in ALP activity and calcium deposits. So far, the biophysical induction of hASC differentiation has been reported by several authors but only in the presence of an induction medium, suggesting that mechanical loading might only boost differentiation. Nevertheless, our data are in line with a recent study demonstrating that mechanical stress alone (mediated by a microstructured nitinol actuator) can induce osteogenic differentiation (Strauß *et al.*, 2012). Some authors have reported that in *in vivo* animal models ESW activated cell proliferation and bone regeneration of segmental defects (Wang *et al.*, 2003) and that the ESW-promoted healing was achieved by stimulation of mesenchymal stem cell recruitment and differentiation into bone-forming cells (Chen *et al.*, 2004b). This is the first report to show the effects of ESW treatment on osteogenic differentiation in an *in vitro* model

using human adipose-derived stem cells and defining the mechanisms involved in the process of differentiation. Recently it has been reported that ESW lead to osteogenic differentiation of bone marrow-derived stem cells via P2X7 (purinergic receptor P2X ligand-gated ion channel 7) signaling (Sun *et al.*, 2013); our data are in good agreement with the effects of ESW observed and add new insights into the mechanisms involved. Moreover, in a recent paper on equine ASCs (Raabe *et al.*, 2013), the authors reported a relevant effect of ESW on ASC proliferation but no significant influence on differentiation; the use of cells of different origin and ESW schedules may at least partially explain the differences observed.

To get insight into the mechanisms of the ESW effect, we investigated ROS production in hASCs. We observed ROS production after only 1 minute from the treatment, regardless of the presence of osteogenic medium. ROS production is involved not only in cellular proliferation but also in differentiation (Kanda *et al.*, 2011; Sauer *et al.*, 2000). Induction of ROS by ESW treatment is in agreement with a previous report demonstrating that O_2^- mediated the ESW-induced ERK activation and osteogenic differentiation of bone marrow mesenchymal stem cells (Wang *et al.*, 2002b). Moreover, ROS production has been found to increase during the differentiation of human mesenchymal stem cells into adipocytes (Tormos *et al.*, 2011). Franceschi *et al*. (2003) reported that the transcription factor Runx2, necessary for osteoblast differentiation and bone formation, is a target of mechanotransduction and it is responsive to multiple pathways, mostly MAPK and BMP2/Smad signaling. Our data confirmed that ESW treatment determined ERK phosphorylation as well as BMP2 expression and Smad phosphorylation. The ERK pathway is reported as a classical signaling pathway that regulates mechanical force-induced up-regulation of osteogenic

differentiation of MSCs (Zhang *et al.,* 2012; Kim *et al.*, 2010) and its phosphorylation is involved in the activation of Runx2 (Franceschi *et al.*, 2007). BMPs are important osteogenic mediators in the regulation of new bone formation (Gazzero *et al.*, 2006). Our data are in line with previous reports demonstrating that ESW treatment increased the expression of BMP2 in experimental models of femur fractures (Wang *et al.*, 2008) and necrotic femoral heads (Ma *et al.*, 2008). Moreover, an increase in serum levels of BMP2 in patients treated with ESW for non-union fractures has been reported (Wang *et al.*, 2009). BMP2/Smad signaling is believed to control Runx2 directly (Phimphilai *et al.*, 2006; Liu *et al.*, 2011); therefore, this pathway can be regarded as a possible mechanism explaining the effect of ESW treatment on Runx2 gene expression that we observed.

Even though we are still far from elucidating all the mechanisms accounting for the effects of ESW in hASCs differentiation into osteoblast-like cells, the results reported in the present paper, in addition to previous data from the literature, define important signaling pathways involved in the mechanotransduction of ESW, as depicted in figure 5. ESW, in particular, determine ROS production and induce ERK phosphorylation. On the one hand, this leads to BMP2 expression and Smad phosphorylation, which, as reported elsewhere (Phimphilai M *et al.*, 2006; Liu *et al.*, 2011), may regulate Runx2 expression. On the other hand, it has been reported that ERK phosphorylates Runx2 (Kanno T *et al.*, 2007; Liu *et al.*, 2011), inducing its transcriptional activity. Hence, both the induced expression of Runx2 and its augmented transcriptional activity explain, at least partially, the effect of ESW treatment on osteogenic differentiation of hASCs and suggest probable mechanisms by which shock waves promote bone healing. Our data suggest a time-dependent cascade of events that starts with ROS production elicited by

ESW and finally comes to a modulation of ALP protein function in terms of phosphatase activity and calcium deposits.

In conclusion, this study represents an important step towards the combination of hASCs and ESW for tissue engineering procedures in the treatment of bone tissue damage. By using stem cells from adipose tissue the ethical problems related to the use of embryonic stem cells will be overcome. However, this is an *in vitro* study and the optimal energy intensity and number of shots are likely to vary in clinical applications, due to the different responses to ESW treatment elicited by different tissues. Additional *in vivo* work will be required to determine the real therapeutic potential of ESW and the set-up of clinical trials will definitively assess the use of ESW as an additional tool for improving the outcome of regenerative treatment.

Acknowledgments: We thank: Loredana Serpe, Department of Drug Science and Technology, University of Turin, Turin, Italy; Anna Teresa Brini, Department of Biomedical, Surgical and Dental Sciences, University of Milan, Milan, Italy; Sebastiano Colombatto, Department of Oncology, University of Turin, Turin, Italy. We thank Med & Sport 2000 S.r.l., Turin, Italy, for providing the shock wave generator. The study was supported by "Progetto Ateneo 2011'', University of Turin, Turin, to Roberto Frairia. Francesca Marano was supported by the "Lagrange Project" from the CRT Foundation, Turin.

Conflict of Interest Statement

None of the authors has commercial or other interests that create conflict with the data presented and analyzed here.

References

Alves EM, Angrisani AT, Santiago MB. 2009; The use of extracorporeal shock waves in the treatment of osteonecrosis of the femoral head: a systematic review. *Clin Rheumatol* **28**:1247-1251.

Canaparo R, Serpe L, Catalano MG, *et al*. 2006; High energy shock waves (HESW) for sonodynamic therapy: effects on HT-29 human colon cancer cells. *Anticancer Res* **26**: 3337-3342.

Chen JM, Hsu SL, Wong T, *et al.* 2009; Functional outcomes of bilateral hip necrosis: total hip arthroplasty versus extracorporeal shockwave. *Arch Orthop Trauma Surg* **129**: 837-841.

Chen YJ, Kuo YR, Yang KD, *et al.* 2004a; Activation of extracellular signal-regulated kinase (ERK) and p38 kinase in shock wave-promoted bone formation of segmental defect in rats. *Bone* **34**: 466-477.

Chen YJ, Wurtz T, Wang CJ, *et al.* 2004b; Recruitment of mesenchymal stem cells and expression of TGF-beta 1 and VEGF in the early stage of shock wave-promoted bone regeneration of segmental defect in rats. *J Orthop Res* **22**: 526-534.

de Girolamo L, Sartori MF, Albisetti W, *et al*. 2007; Osteogenic differentiation of human adipose-derived stem cells: comparison of two different inductive media. *J Tissue Eng Regen Med* **1**: 154-157.

Elster EA, Stojadinovic A, Forsberg J, *et al.* 2010; Extracorporeal shock wave therapy for nonunion of the tibia. *J Orthop Trauma* **24**: 133-141.

Frairia R, Catalano MG, Fortunati N, *et al*. 2003; High energy shock waves (HESW) enhance paclitaxel cytotoxicity in MCF-7 cells. *Breast Cancer Res Treat* **81**: 11-19.

Franceschi RT and Xiao G. 2003; Regulation of the osteoblast-specific transcription factor, Runx2: responsiveness to multiple signal transduction pathways. *J Cell Biochem* **88**: 446-454.

Franceschi RT, Ge C, Xiao G, *et al*. 2007; Transcriptional regulation of osteoblasts. *Ann N Y Acad Sci* **1116**: 196-207.

Gazzerro E and Canalis E. 2006; Bone morphogenetic proteins and their antagonists. Rev *Endocr Metab Disord* **7**:51-65.

Kanda Y, Hinata T, Kang SW *et al*. 2011; Reactive oxygen species mediate adipocyte differentiation in mesenchymal stem cells. *Life Sci* **89**: 250-258.

Kanno T, Takahashi T, Tsujisawa T, *et al.* 2007; Mechanical stress-mediated Runx2 activation is dependent on Ras/ERK1/2 MAPK signaling in osteoblasts. *J Cell Biochem* **101**:1266–1277.

Kim IS, Song YM, Hwang SJ. 2010; Osteogenic responses of human mesenchymal stromal cells to static stretch. *J Dent Res* **89**: 1129-1134.

Komuro I, Kudo S, Yamazaki T, et al. 1996; Mechanical stretch activates the stress-activated protein kinases in cardiac myocytes. *Faseb J* 10: 631–636.

Liu L, Shao L, Li B, et al. 2011; Extracellular signal-regulated kinase1/2 activated by fluid shear stress promotes osteogenic differentiation of human bone marrow-derived mesenchymal stem cells through novel signaling pathways. *Int J Biochem Cell Biol* **43**:1591-601.

Ma HZ, Zeng BF, Li XL, *et al.* 2008; Temporal and spatial expression of BMP-2 in sub-chondral bone of necrotic femoral heads in rabbits by use of extracorporeal shock waves. *Acta Orthop* **79**: 98-105.

Maroni P, Brini AT, Arrigoni E, *et al.* 2012; Chemical and genetic blockade of HDACs enhances osteogenic differentiation of human adipose tissue-derived stem cells by oppositely affecting osteogenic and adipogenic transcription factors. *Biochem Biophys Res Commun* **428**: 271-277.

Maul TM, Chew DW, Nieponice A, *et al.* 2011; Mechanical stimuli differentially control stem cell behavior: morphology, proliferation, and differentiation. *Biomech Model Mechanobiol* **10**: 939-953.

Muzio G, Vernè E, Canuto RA, *et al.* 2010; Shock Waves Induce Activity of Human Osteoblast Like Cells in Bioactive Scaffolds. *J Trauma* **68**: 1439-1444.

Phimphilai M, Zhao Z, Boules H, *et al.* 2006; BMP signaling is required for RUNX2-dependent induction of the osteoblast phenotype. *J Bone Miner Res.* **21**(4):637-46.

Pountos I and Giannoudis PV. 2005; Biology of mesenchymal stem cells. *Injury* **36:** S8–S12.

Qin L, Wang L, Wong MW, *et al.* 2010; Osteogenesis induced by extracorporeal shockwave in treatment of delayed osteotendinous junction healing. *J Orthop Res* **28**: 70-76.

Raabe O, Shell K, Goessl A, *et al.* 2013; Effect of extracorporeal shock wave on proliferation and differentiation of equine adipose tissue-derived mesenchymal stem cells in vitro. *Am J Stem Cell* **2**: 62-73.

Rauch C and Loughna PT. 2008; Stretch-induced activation of ERK in myocytes is p38 and calcineurin-dependent. *Cell Biochem Funct* **26**:866-869.

Rompe JD, Rosendahl T, Schöllner C, et al. 2001; High-energy extracorporeal shock wave treatment of nonunions. *Clin Orthop* **387**:102-111.

Sauer H, Rahimi G, Hescheler J, *et al.* 2000; Role of reactive oxygen species and phosphatidylinositol 3-kinase in cardiomyocyte differentiation of embryonic stem cells. *FEBS Lett* **476**: 218-223.

Soucacos PN, Johnson EO, Babis G. 2008; An update on recent advances in bone regeneration. *Injury* **39**: S1-4.

Strauß S, Dudziak S, Hagemann R, *et al.* 2012; Induction of Osteogenic Differentiation of Adipose Derived Stem Cells by Microstructured Nitinol Actuator-Mediated Mechanical Stress. *PLoS ONE* **7**: e51264.

Sturtevant B. 1996; 'Shock waves physic of lithotriptors' in *Smith's Textbook of endourology.* Smith A, Badlani GH, Bagley DH, eds, St Louis, MO, Quality Medical Publishing; 529-552.

Sun D, Junger WG, Yuan C, *et al.* 2013; Shockwaves Induce Osteogenic Differentiation of Human Mesenchymal Stem Cells through ATP Release and Activation of P2X7 Receptors. *Stem Cells* doi: 10.1002/stem.1356.

Tischer T, Milz S, Weiler C, *et al.* 2008; Dose-dependent new bone formation by extracorporeal shock wave application on the intact femur of rabbits. *Eur Surg Res* **41**:44-53.

Tormos KV, Anso E, Hamanaka RB, *et al.* 2011; Mitochondrial complex III ROS regulate adipocyte differentiation. *Cell Metab* **14**: 537-544.

van der Jagt OP, Piscaer TM, Schaden W, *et al.* 2011; Unfocused extracorporeal shock waves induce anabolic effects in rat bone. J Bone Joint Surg Am **93**: 38-48.

van der Jagt OP, Waarsing JH, Kops N, et al. 2013; Unfocused extracorporeal shock waves induce anabolic effects in osteoporotic rats. *J Orthop Res* **31**:768-775.

Wang CJ, Chen HS, Chen CE, et al. 2001; Treatment of nonunions of long bone fractures with shock waves. *Clin Orthop Rel Res* **387**:95-101.

Wang CJ, Huang CC, Wang JW, *et al.* 2012b; Long-term results of extracorporeal shockwave therapy and core decompression in osteonecrosis of the femoral head with eight- to nine-year follow-up. *Biomed J* 35:481-485.

Wang CJ, Wang FS, Yang KD. 2008; Biological effects of extracorporeal shockwave in bone healing: a study in rabbits. *Arch Orthop Trauma Surg* **128**: 879-884.

Wang CJ, Yang KD, Ko JY, *et al.* 2009; The effects of shockwave on bone healing and systemic concentrations of nitric oxide (NO), TGF-beta1, VEGF and BMP-2 in long bone non-unions. *Nitric Oxide* **20**: 298-303.

Wang CJ. 2012a; Extracorporeal shockwave therapy in musculoskeletal disorders. *J Orthop Surg Res* **7**: 11.

Wang FS, Wang CJ, Sheen-Chen SM, *et al.* 2002b; Superoxide mediates shock wave induction of ERK-dependent osteogenic transcription factor (CBFA1) and mesenchymal cell differentiation toward osteoprogenitors. *J Biol Chem* **277**: 10931-10937.

Wang FS, Yang KD, Chen RF, *et al.* 2002a; Extracorporeal shock wave promotes growth and differentiation of bone-marrow stromal cells towards osteoprogenitors associated with induction of TGF-beta1. *J Bone Joint Surg Br* **84**:457-461.

Wang FS, Yang KD, Kuo YR, *et al.* 2003; Temporal and spatial expression of bone morphogenetic proteins in extracorporeal shock wave-promoted healing of segmental defect. *Bone* **32**: 387-396.

Xu ZH, Jiang Q, Chen DY, *et al.* 2009; Extracorporeal shock wave treatment in nonunions of long bone fractures. *Int Orthop* **33**:789-793.

Zhang P, Wu Y, Jiang Z, *et al.* 2012; Osteogenic response of mesenchymal stem cells to continuous mechanical strain is dependent on ERK1/2-Runx2 signaling. *Int J Mol Med* **29**: 1083-1089.

Zuk PA, Zhu M, Mizuno H, *et al.* 2001; Multilineage cells from human adipose tissue: implications for cell-based therapies. *Tissue Eng* **7**: 211-228.

Table 1 Primers for real-time PCR

Runx2	Sense: 5’- CGG AGT GGA CGA GGC AAG AG-3’ Antisense: 5’- AGG CGG TCA GAG AAC AAA CTA GG -3’
ALP	Sense: 5’- ATG AGG CGG TGG AGA TGG AC -3’ Antisense: 5’- CAT ACA GGA TGG CAG TGA AGG G -3’
BMP2	Sense: 5’- CGG GAG AAG GAG GAG GCA AAG -3’ Antisense: 5’- GAA GCA GCA ACG CTA GAA GAC AG -3’
β-ACT	Sense: 5’- GCG AGA AGA TGA CCC AGA TC- 3’ Antisense: 5’- GGA TAG CAC AGC CTG GAT AG-3’
β2-microglobulin	Sense: 5’-AGA TGA GTA TGC CTG CCG TGT G-3’ Antisense: 5’-TCA ACC CTC CAT GAT GCT GCT TAC-3’
L13A	Sense: 5’-GCA AGC GGA TGA ACA CCA ACC-3’ Antisense: 5’-TTG AGG GCA GCA GGA ACC AC-3’

Figure Legends

Figure 1. Effects of ESW and osteogenic medium on Runx2 (A) and ALP (B) gene expression. mRNA expression was evaluated by RT-PCR after 72 hours from treatments. Results are normalized for three different housekeeping genes (β-actin, β2-microglobulin and L13A) and expressed as relative expression fold *vs* lower level of expression. **Effects of osteogenic medium and ESW on ALP activity (C):** Enzymatic activity at day 6 was calculated as units normalized for total protein content (U/μg protein) and expressed as ratio *vs* DMEM. Level of significance *vs* DMEM: *, $p<0.05$; **, $p<0.01$; ***, $p<0.001$; level of significance *vs* no ESW: °, $p<0.05$; °°, $p<0.01$.

Figure 2. Effect of ESW and osteogenic medium on calcium deposition. (A): Calcium deposits at 28 days (arrows) as revealed by Alizarin Red Staining. Magnification 400x. I: DMEM; II: DMEM ESW; III: OST; IV: OST ESW. **(B):** Staining quantification was normalized for DNA content and expressed as ratio *vs* DMEM. Level of significance *vs* DMEM: **, $p<0.01$; ***, $p<0.001$; level of significance *vs* no ESW: °, $p<0.05$; °°, $p<0.01$.

Figure 3. Effects of ESW on ROS formation (A): Intracellular ROS levels measured using a flow cytometer. Level of significance *vs* no ESW: ***, $p<0.001$. **Effects of ESW on ERK1/2 phosphorylation (B):** ERK phosphorylation in either DMEM or osteogenic medium, after EWS treatment (upper panel). Total ERK 1/2 was evaluated in order to check the amount of loaded protein (lower panel). Histograms: semiquantitative analysis of Western blot results after 15' and 60'. Level of significance *vs* no ESW: *, $p<0.05$.

Figure 4. Effects of ESW and osteogenic medium on BPM2 expression (A): mRNA expression was evaluated with RT-PCR. Results are normalized for three different

housekeeping genes (β-actin, β2-microglobulin and L13A) and expressed as relative expression fold *vs* lower level of expression. Level of significance *vs* DMEM: *** $p<0.001$; level of significance *vs* no ESW: °°° $p<0.001$. **Effects of ESW on Smad localization (B) and phosphorylation (C):** Immunofluorescence for total-Smad (B) and phospho-Smad (C) was performed on cells either in basal conditions or in osteogenic medium after ESW treatment. Magnification 400x. I: DMEM; II: DMEM ESW; III: OST; IV: OST ESW.

Figure 5. Signal transduction pathways involved in osteoblast differentiation by ESW treatment. Shock waves determine ROS production that induces ERK phosphorylation, as also reported by Wang *et al.* (2002b). This event leads to BMP2 expression, followed by Smad 1/5/8 phosphorylation. Autocrine BMP2 signaling with consequent Smad phosphorylation may guide Runx2 expression (Phimphilai *et al.*, 2006; Liu *et al.*, 2011). Finally, ERK can also phosphorylate Runx2 inducing its transcriptional activity (Kanno *et al.*, 2007; Liu *et al.*, 2011) that leads to ALP expression and activity.

Table 1 Primers for real-time PCR

Runx2	Sense: 5'- CGG AGT GGA CGA GGC AAG AG-3' Antisense: 5'- AGG CGG TCA GAG AAC AAA CTA GG -3'
ALP	Sense: 5'- ATG AGG CGG TGG AGA TGG AC -3' Antisense: 5'- CAT ACA GGA TGG CAG TGA AGG G -3'
BMP2	Sense: 5'- CGG GAG AAG GAG GAG GCA AAG -3' Antisense: 5'- GAA GCA GCA ACG CTA GAA GAC AG -3'
β-ACT	Sense: 5'- GCG AGA AGA TGA CCC AGA TC- 3' Antisense: 5'- GGA TAG CAC AGC CTG GAT AG-3'
β2-microglobulin	Sense: 5'-AGA TGA GTA TGC CTG CCG TGT G-3' Antisense: 5'-TCA ACC CTC CAT GAT GCT GCT TAC-3'
L13A	Sense: 5'-GCA AGC GGA TGA ACA CCA ACC-3' Antisense: 5'-TTG AGG GCA GCA GGA ACC AC-3'

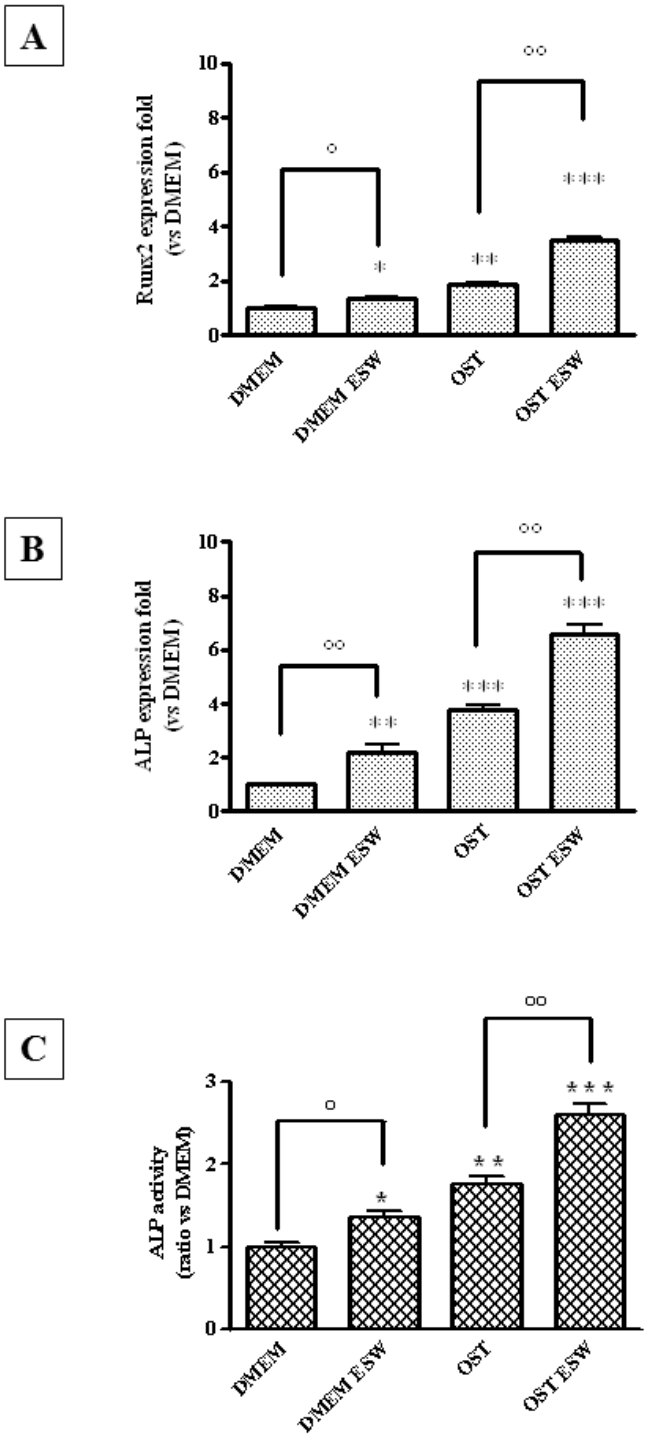
A
Runx2 expression fold
(vs DMEM)
10
8
6
4
2
0
°
°°
*
**
***
DMEM
DMEM ESW
OST
OST ESW
B
ALP expression fold
(vs DMEM)
10
8
6
4
2
0
°°
**
***
***
DMEM
DMEM ESW
OST
OST ESW
C
ALP activity
(ratio vs DMEM)
3
2
1
0
°
°°
*
**
***
DMEM
DMEM ESW
OST
OST ESW

Fig 1

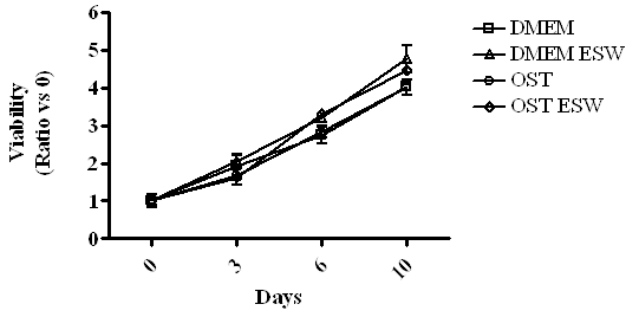

Suppl.Fig 1

Supplementary figure 1. Effect of osteogenic medium and ESW cell viability. At, 3, 6 and 10 days after treatment, cell viability was determined by the WST-1 method, and expressed as ratio *vs* day 0 (DMEM).